THE JOURNAL OF PHYSICAL CHEMISTRY A

Article

pubs.acs.org/JPCA

# pH Oscillations and Mechanistic Analysis in the Hydrogen Peroxide−Sulfite−Thiourea Reaction System

Ling Yuan, Tao Yang, Yang Liu, Ying Hu, Yuemin Zhao, Juhua Zheng, and Qingyu Gao*

College of Chemical Engineering, China University of Mining and Technology, Xuzhou 221116, P. R. China

**ABSTRACT:** A new pH oscillator has been constructed by combining the pH clock reaction $H_2O_2$−$SO_3^{2-}$−$H^+$ with thiourea (Tu, $(NH_2)_2CS$) as a proton-consuming species. The system exhibited oligo-oscillatory behavior in a closed system, and large amplitude oscillations in a continuous-flow stirred tank reactor (CSTR) were observed in a narrow range of input concentrations, flow rate, and temperature. For the purpose of constructing the kinetic model, a reversed-phase ion-pair high-performance liquid chromatography (HPLC) and mass spectrometer (MS) were used to track and determine intermediate species during the oxidation of thiourea by hydrogen peroxide. Experimental results illustrated that the four species: thiourea monoxide (TuO), formamidine disulfide ($Tu_2^{2+}$), thiourea dioxide ($TuO_2$), and thiourea trioxide ($TuO_3$) were formed during the oxidation process. A ten-step mechanistic model was proposed, where TuO was another key species participating in two proton feedback loops in addition to bisulfite. Numerical simulations based on this model agreed well with the experimental results.

pH Oscillations

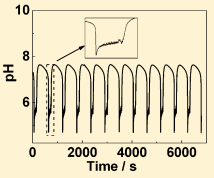


Species by HPLC

| pH | $Tu_2^{2+}$ | TuO | $TuO_2$ | $TuO_3$ |
|---|---|---|---|---|
| 2.0 | √ | √ | √ | √ |
| 3.0 | √ | √ | √ | √ |
| 5.0 | X | √ | √ | √ |
| 7.11 | X | √ | √ | √ |

## 1. INTRODUCTION

The pH oscillator is one of the important branches of the whole oscillatory family, in which the pH value as a driving force oscillates rhythmically. Since Orbán and Epstein discovered the first pH oscillator in the reaction between hydrogen peroxide and sulfide ion,[1] the family of pH oscillators has grown rapidly. As of now, there are about dozens of pH oscillating reactions in the family. A simple model proposed by Rábai summarized a typical chemical mechanism for pH oscillators:[2]

$$A + H^+ \leftrightarrow AH \quad (R1)$$

$$AH + H^+ + B \rightarrow 2H^+ + P^- \quad (R2)$$

$$H^+ + C^- \rightarrow Q \quad (R3)$$

The model contains a fast protonation equilibrium process R1, an autocatalytic production of protons R2, and a proton consuming process R3, where A is a reducing agent and B is an oxidant. Autocatalytic reactions R2, as a prototype of positive feedbacks, play a central role in pH oscillatory systems. In the experiment, sulfite ions are most often used as component A, while the typical oxidant B is $IO_3^-$, $BrO_3^-$, or $H_2O_2$. A large number of pH oscillatory reactions have been developed by coupling appropriate negative feedbacks to the autocatalytic reaction using $S_2O_3^{2-}$,[3,4] $HCO_3^-$,[5,6] $Fe(CN)_6^{4-}$,[7−9] thiourea (Tu),[10] or $Mn^{2+}$.[11]

Among the above agents for negative feedback, Tu, a typical sulfur containing compound, is of high industrial value, being widely used in the hydrometallurgy and textile industry. In addition, oxidation of Tu by oxyhalogens such as $IO_3^-$,[12] $BrO_3^-$,[13] and $ClO_2^-$[14] in acidic aqueous solution exhibits exotic kinetics. Especially, the reaction between $ClO_2^-$ and Tu has been found to give rise to complex nonlinear behaviors such as mixed-mode oscillations and chemical chaos in a continuous-flow stirred tank reactor (CSTR).[14] Furthermore, in the $IO_3^-$−$SO_3^{2-}$−Tu reaction system, Tu can also be used to consume protons and make the system display complex pH oscillations in a CSTR.[10,15] All of the above, the kinetic mechanism and simulation of oscillations, chaos, and spatiotemporal patterns, remain as open questions.

An important purpose of constructing pH oscillators is to explore complex spatiotemporal self-organization. After the first experimental demonstration of the reaction-diffusion pattern in the pH oscillatory system ($IO_3^-$−$SO_3^{2-}$−$Fe(CN)_6^{4-}$) was discovered in 1993,[16] the number of spatiotemporal systems stagnated for nearly 20 years. Recently, De Kepper and his co-workers have proposed a semiempirical method for designing reaction-diffusion patterns for the pH regulated system in the one-side-fed reactor (OSFR),[17,18] which increased the number of spatiotemporal systems to five. However, more work[19,20] is required to optimize pH oscillators for studying complex spatiotemporal patterns such as consistence of coherence and incoherence[21−23] and biomimetic dynamics in responsive gel.[24]

The halogen free reaction between $H_2O_2$ and $SO_3^{2-}$ (HPS reaction) is a typical pH-clock reaction, which can be described by the following chemical steps R4 and R5:

$$H^+ + SO_3^{2-} \leftrightarrow HSO_3^- \quad (R4)$$

$$H_2O_2 + HSO_3^- \rightarrow H^+ + SO_4^{2-} + H_2O \quad (R5)$$

This HPS reaction system exhibits bistability between an alkaline (pH = 8−9) unreacted state branch and an acidic (pH = 4−5) reacted state branch in a CSTR. According to the above

**Received:** January 19, 2014
**Revised:** March 21, 2014
**Published:** March 24, 2014

general model, this autocatalytic reaction should be supplemented by a negative feedback reaction to provide sustained pH oscillations. The negative feedback reaction has included two sources, which are the nonredox reaction and redox reaction. Hydrogen carbonate and carbonate provided a nonredox reaction to remove protons through the equilibrium reactions R6 and R7.[5,25] With regard to the redox reaction, the oxidation of thiosulfate[4] and ferrocyanide[9] by hydrogen peroxide could also consume protons.

$$HCO_3^- + H^+ \leftrightarrow H_2CO_3 \quad \text{(R6)}$$

$$H_2CO_3 \leftrightarrow CO_2(aq) + H_2O \quad \text{(R7)}$$

More recently, pattern formation in the HPS reaction system has been of interest. Sustained and nonsustained reaction-diffusion patterns have been obtained in the HPS-based system combined with $HCO_3^-$ and $Fe(CN)_6^{4-}$.[26,27]

The oxidation of Tu and Tu oxides by $H_2O_2$ in acidic media has been studied.[28−31] The reaction between $H_2O_2$ and Tu could remove protons and produce formamidine disulfide ($Tu_2^{2+}$), providing a negative feedback. Therefore, if Tu is added to the HPS reaction, the combined system (HPSTu) could display large pH oscillations. Also, further oxidation and hydrolysis reactions of $TuO_x$ producing another $H^+$ positive feedback can induce complex pH oscillations. The new pH oscillators might be used as the driving medium in periodic drug-delivery systems[32,33] and DNA-based nanodevices,[34,35] or for investigating reaction-diffusion pattern formation. For the present, batch and CSTR experiments were carried out systematically on the HPSTu reaction system, while HPLC and MS were also employed to track and determine intermediate species during the oxidation processes between $H_2O_2$ and Tu.

## 2. EXPERIMENTAL SECTION

**Materials.** Analytical reagent grade $H_2O_2$ (30%, Sinopharm Chemical Regants), $H_2SO_4$ (Sinopharm Chemical Regants), Tu (99%, Sinopharm Chemical Regants), and $Na_2SO_3$ (98%, Alfar-Aesar) were used without further purification. The deionized water was boiled for 30 min and deoxygenated with bubbling nitrogen for preparing solutions. The concentration of diluted $H_2O_2$ used in the experiments was determined by potassium permanganate titration.

**Batch and CSTR Experiments.** All batch reactions were carried out in a 25.0 mL thermostatted glass vessel. Appropriate volumes of sulfuric acid and sulfite solutions were first mixed, then Tu solution was added, and the reaction was started by adding the hydrogen peroxide solution. The reaction mixture was stirred with a magnetic stirrer (IKA, German). The flow experiments were carried out in a thermostatted flow reactor with the liquid volume of 27.0 mL. The four reagents stored in four vessels were pumped into the reactor by a four-channel peristaltic pump (ISMATEC, Switzerland), respectively. The $H_2O_2$ and Tu solutions entered the CSTR through a single port, while $Na_2SO_3$ and $H_2SO_4$ feed streams were premixed in a premixing head before their entry into the reactor to successfully avoid local acidification. In order to avoid the influence of temperature fluctuation during the reaction, the four inlet tubes were wrapped in a water bath with a constant temperature before entering the CSTR, which made the temperature the same for the entering and reactor solutions. The reaction temperature was maintained by a circulating water pump (PolyScience Instrument, USA). Both the batch reactor and flow reactor were equipped with a pH combined electrode (Cole Parmer, USA) and a thermistor to measure pH and temperature, respectively. The pH−time data were collected with an e-coder 201 (eDAQ, Australia) and recorded by a PC computer.

**HPLC and HPLC−MS Measurement.** HPLC separation experiments were conducted on a Dionex Summit System equipped with a multiple wavelength detector (MWD) and Phenomenex Gemini $C_{18}$ column (5 $\mu$m, 250 × 4.6 mm i.d.). The mobile phase was composed of 0.5 mM phosphate buffer solution containing 2.5 mM tetrabutylammonium hydroxide (TBAOH), as ion-pair agent, and methanol at higher pH (pH > 4). The separation performance was optimized to a ratio of 95:5 ($\nu_{buffer}/\nu_{methanol}$), and the flow rate was set to be 0.5 mL/min. At lower pH (pH < 4), the mobile phase composition was changed to methanol, acetonitrile, and buffer adjusted by hydrochloric acid with the volume ratio of 6:26:68. The flow rate was changed to 0.4 mL/min. The pH of the mobile phase was adjusted to be the same as that of the reaction solution. For each analysis, the injection volume was 10 $\mu$L.

For the sake of determining the intermediates of Tu, the HPLC column effluent was interfaced with an LCQ Advantage ion-trap mass spectrometer (Thermo Finnigan, Waltham, MA) equipped with an electrospray ionization (ESI) ion source. The flow rates of sheath gas and auxiliary/sweep gas were set to be 30 and 10 arbitrary units (arb), respectively, and the temperature of the ion-transfer capillary was 350 °C. The probe voltage was kept at +3.0 kV in positive-ion mode. The reaction was conducted in an enclosed glass vessel lying in a water bath, which kept the reaction temperature at 25 °C. For eliminating oxygen effect, the buffered solutions were bubbled with nitrogen gas for two hours and followed by sampling under nitrogen atmosphere to avoid the effect of oxygen.

**Computation.** The simulations were carried out with a commercial software package (Berkeley Madonna, semi-implicit Runge−Kutta algorithm with error control parameter set at $10^{-10}$) for stiff differential equations. The same results were obtained with the error control parameter set at $10^{-6}$ and $10^{-12}$ and with the Gear algorithm.

## 3. RESULTS AND DISCUSSION

First of all, the HPSTu reaction system was investigated in batch. Then the experiments and simulation for the mixed system were carried out in a CSTR. In addition, HPLC combined with mass spectrometry was used to determine the intermediates during the oxidation of Tu by $H_2O_2$ for mechanistic analysis.

**Experiments in Closed System.** It is important to determine whether Tu could play the negative-feedback role in the HPS reaction system in our flow experiments. With this problem, a series of kinetic batch runs was carried out in the HPSTu reaction system during which the pH change was tracked. The results are illustrated in Figure 1. Under the closed conditions, the HPS reaction system displayed typical proton autocatalysis curves as in the broken line of Figure 1. With Tu as a negative-feedback agent, the reaction showed oligo-oscillatory behavior in a closed system.

As shown in the solid line of Figure 1, the batch run contains three stages. At the beginning of the reaction, the initial pH value of the system is about 8.5 because of the fast protonation process. Under these conditions the autocatalytic reaction is gradually enhanced (R5), resulting in a decrease in pH. In the second stage of the reaction, Tu is oxidized to thiourea


dx.doi.org/10.1021/jp500627z | J. Phys. Chem. A 2014, 118, 2702−2708

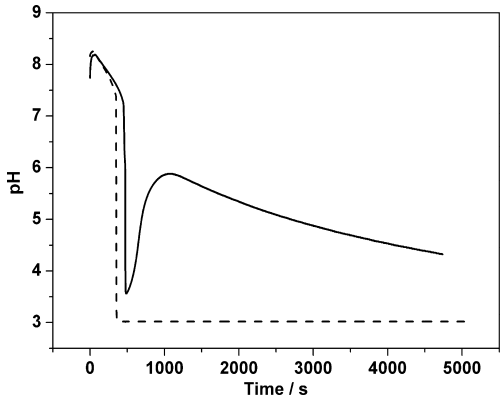


**Figure 1.** pH vs time curves in closed system: $[H_2O_2]_0$ = 25 mM, $[SO_3^{2-}]_0$ = 14 mM, $[H_2SO_4]_0$ = 0.3 mM, $T$ = 20.0 °C, stirred rate = 800 rpm, and $[Tu]_0$ = broken line, 0 mM; solid line, 2 mM.

monoxide (TuO) by $H_2O_2$ (R8). The TuO is a key intermediate product, which facilitates the negative feedback process (R9) to consume two protons and make pH rise, approaching pH = 6. However, as the pH increases, $Tu_2^{2+}$ could dissociate, which means that R9 is a reversible reaction. In the third stage of the reaction, oxidation of TuO by excess $H_2O_2$ occurs through oxygen additions on sulfur, with subsequent formation of thiourea dioxide ($TuO_2$), thiourea trioxide ($TuO_3$), and two protons (R10). Simultaneously, $TuO_3$ could also hydrolyze slowly to bisulfite, which drives the slow pH decrease in the third reaction stage (R11 and R5).

$$H_2O_2 + Tu \rightarrow TuO + H_2O \quad \text{(R8)}$$

$$Tu + TuO + 2H^+ \leftrightarrow Tu_2^{2+} + H_2O \quad \text{(R9)}$$

$$TuO \xrightarrow{H_2O_2} TuO_2 \xrightarrow{H_2O_2} TuO_3 \xrightarrow{H_2O_2} SO_4^{2-} + \text{urea} + 2H^+ \quad \text{(R10)}$$

$$TuO_3 + H_2O \rightarrow HSO_3^- + \text{urea} + H^+ \quad \text{(R11)}$$

**Experiments under Flow Conditions.** We performed a series of experiments in a CSTR, in which the reactant concentrations and other experimental constraint parameters were varied. Through this way, the conditions for sustained pH oscillations were systematically investigated. A typical time series is shown in Figure 2. The pH change can be as large as 3 units, ranging from 4.7 to 7.7. There are a number of tiny and irregular small-amplitude oscillations within the pH range 5.5–5.7 along the pH rising profile, which can be seen from the enlarged view in Figure 2. The reaction system is extremely sensitive to the temperature fluctuation. Therefore, the reaction temperature must be carefully controlled. The oscillations only occurred in a narrow temperature range from 27.9 to 31.0 °C. Below 27.9 °C and above 31.0 °C there is no observed oscillatory behavior at our given initial concentrations. The pH–time series were obtained at different temperatures when other parameters were fixed as shown in Figure 3. Obviously, the period length decreased with increasing temperature, so there is no temperature compensation in this system.

During the experiments, the concentrations of hydrogen peroxide and sulfite were fixed at 25 and 14 mM, respectively. We obtained the phase diagrams in the flow rate–$[Tu]_0$ and flow rate–$[H_2SO_4]_0$ planes as shown in Figure 4a,b, respectively. Oscillations occurred in a very narrow range of flow rate and initial concentrations of Tu and sulfuric acid.

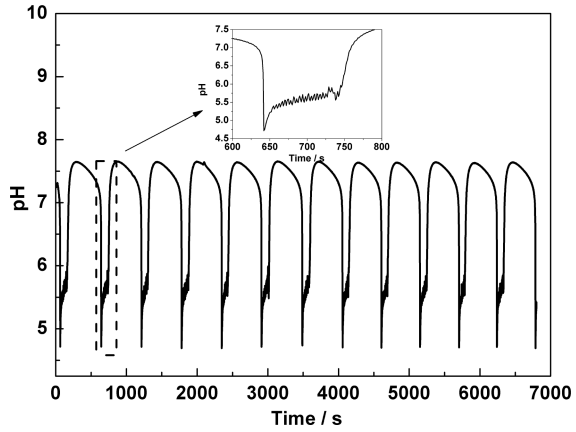


**Figure 2.** Sustained pH oscillations in a CSTR. Input concentrations: $[H_2O_2]_0$ = 25 mM, $[SO_3^{2-}]_0$ = 14 mM, $[H_2SO_4]_0$ = 0.25 mM, $[Tu]_0$ = 2 mM, $T$ = 27.9 °C, $k_0 = 8.33 \times 10^{-4}$ s$^{-1}$, and stirred rate = 800 rpm.

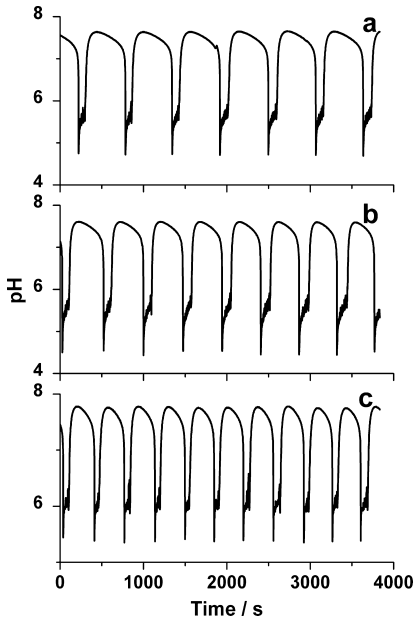


**Figure 3.** Measured pH oscillations in a CSTR at different temperatures. Input concentrations: $[H_2O_2]_0$ = 25 mM, $[SO_3^{2-}]_0$ = 14 mM, $[H_2SO_4]_0$ = 0.25 mM, $[Tu]_0$ = 2 mM, $k_0 = 8.33 \times 10^{-4}$ s$^{-1}$, and stirred rate = 800 rpm. $T$ = a, 27.9 °C; b, 30.1 °C; c, 30.9 °C.

**Species Analysis during $H_2O_2$–Tu Reaction.** In order to identify the species formed during the reaction, a series of experiments were followed online by HPLC and MS. Four sulfur-containing intermediates were detected existing in the reaction system in low pH conditions, including $Tu_2^{2+}$, TuO, $TuO_2$, and $TuO_3$. Table 1 presents the intermediates by HPLC at different pH. The chromatograms at different reaction times at pH = 2.0 and 5.0 are shown in Figure 5a,b, respectively. As shown in Table 1 and Figure 5, $Tu_2^{2+}$ can only be monitored by HPLC in low pH conditions because it is unstable in higher pH and undergoes significant hydrolysis with a half-life period of 40 and 6.7 s at pH = 4.93 and 6.09, respectively.[36] Meanwhile, the HPLC–MS method was used to prove the existence of TuO and $Tu_2^{2+}$. Figure 6a is the total ion chromatogram in positive-ion mode, which indicates that there are three chromatographic species eluted at 5.1, 5.8, and 6.98 min. The corresponding mass spectra of the three species are given in Figure 6b–d, respectively. From the mass spectra, the three species should be


dx.doi.org/10.1021/jp500627z | J. Phys. Chem. A 2014, 118, 2702–2708

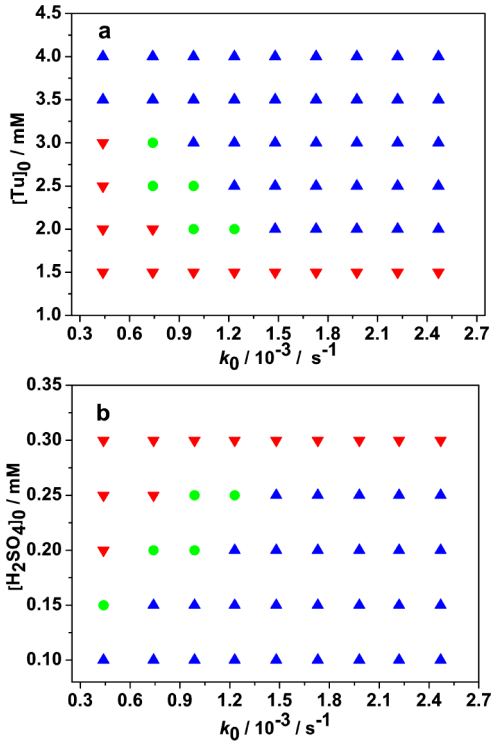


**Figure 4.** Phase diagrams in the flow rate−$[Tu]_0$ and flow rate−$[H_2SO_4]_0$ planes. Fixed parameters: $[H_2O_2]_0$ = 25 mM, $[SO_3^{2-}]_0$ = 14 mM; a, $[H_2SO_4]_0$ = 0.25 mM; b, $[Tu]_0$ = 2 mM; $T$ = 28.0 °C, and stirred rate = 800 rpm. ▲, high pH state; ●, oscillatory state; and ▼, low pH state.

**Table 1. Intermediates at Different pH**

| pH | $Tu_2^{2+}$ | TuO | $TuO_2$ | $TuO_3$ |
|---|---|---|---|---|
| 2.0 | √ | √ | √ | √ |
| 3.0 | √ | √ | √ | √ |
| 5.0 | × | √ | √ | √ |
| 7.11 | × | √ | √ | √ |

$Tu_2^{2+}$ ($[M + H]^+$ = 151.3, $[M + MeOH + H]^+$ = 183.5, and $[M + ACN + H]^+$ = 191.9), TuO ($[M + H]^+$ = 93.3 and $[M + ACN + H]^+$ = 134.1), and Tu ($[M + H]^+$ = 77.2 and $[M + ACN + H]^+$ = 118.0). The inset picture of Figure 6c is the second order mass spectrum of $m/z$ 93.1. The $m/z$ 75 peak should be the fragment of $[TuO + H]^+$ removed by a $H_2O$.

**Mechanistic Analysis and Simulation.** A mechanistic model in Table 2 was developed to explain the complex kinetics, which consists of ten steps including two protonation equilibria, seven redox reactions, and a hydrolysis reaction. Those reactions, rate laws, and rate constants are given in Table 2. Reaction M3, oxidation of bisulfite, is known to be autocatalytic in $H^+$, for which the rate equation and rate constants can be found in ref 4. The oxidation of sulfite should be included for the pH range of the kinetic curves. The oxidation of Tu by $H_2O_2$ is very complex because these reactions are known to yield a variety of intermediates, including $Tu_2^{2+}$, TuO, $TuO_2$, and $TuO_3$, leading to the product of complete oxidation, sulfate.[29] Reaction M5, being of first kinetic order with respect to $H_2O_2$ and Tu, respectively, could produce TuO, which could react with Tu (M6) to consume protons. Meanwhile, TuO could be further oxidized by $H_2O_2$ through M7−M9 leading to regeneration of the protons. It is well-known that $Tu_2^{2+}$ is unstable at high pH (>3), so M6 should be reversible and pH dependent. The rate law for the M6 forward reaction can be expressed in two parts, consisting of $k_6[Tu][TuO]$ and $k_6'[H^+][Tu][TuO]$.

$$v_6 = (k_6 + k_6'[H^+])[Tu][TuO] \quad \text{(E1)}$$

Since no independent experimental rate constants for reaction M6 are available, they were chosen by fitting the calculated curves to the measured ones.

Figure 7a shows the peak area-time curves for TuO on HPLC at a pH range of 1.5−2.75. With increasing pH, TuO is consumed more quickly. The following linear relationship between rate law and $[OH^-]$ was obtained for M7 from Figure 7b.

$$v_7 = (k_7 + k_7'[OH^-])[H_2O_2][TuO] \quad \text{(E2)}$$

Experimental values of $k_7$ and $k_7'$ are $1.28 \times 10^{-4}$ $M^{-1}$ $s^{-1}$ and $2.96 \times 10^8$ $M^{-2}$ $s^{-1}$, respectively. For simulating pH oscillations, we used $k_7' = 1.092 \times 10^6$ $M^{-2}$ $s^{-1}$ rather than the experimental result. This disparity is possibly because both temperature and pH during the CSTR experiments are higher than those during HPLC determination.

According to E1 and E2, at the low pH of oscillations the M6 forward reaction consumes protons, resulting in negative feedback and corresponding pH rise. However, at high pH, the reversible M6 reaction moves backward and TuO can be oxidized through M7−M9. These reactions, in addition to M3, produce protons and make the pH drop. So, multiple proton processes (M3, M6, M−6, M7−M9) could produce complex

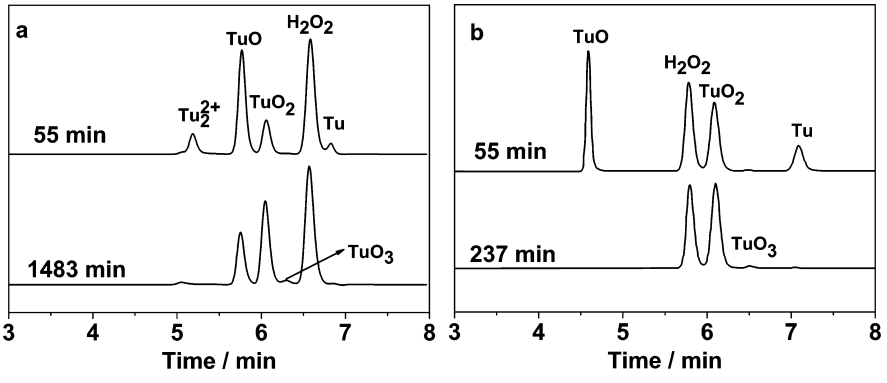


**Figure 5.** Chromatograms at different reaction times during the $H_2O_2$−Tu system. a, pH = 2.0, $[H_2O_2]_0/[Tu]_0$ = 40:1; b, pH = 5, $[H_2O_2]_0/[Tu]_0$ = 20:1. $[Tu]_0$ = 0.5 mM, $T$ = 25 °C, and $\lambda$ = 214 nm.


dx.doi.org/10.1021/jp500627z | J. Phys. Chem. A 2014, 118, 2702−2708

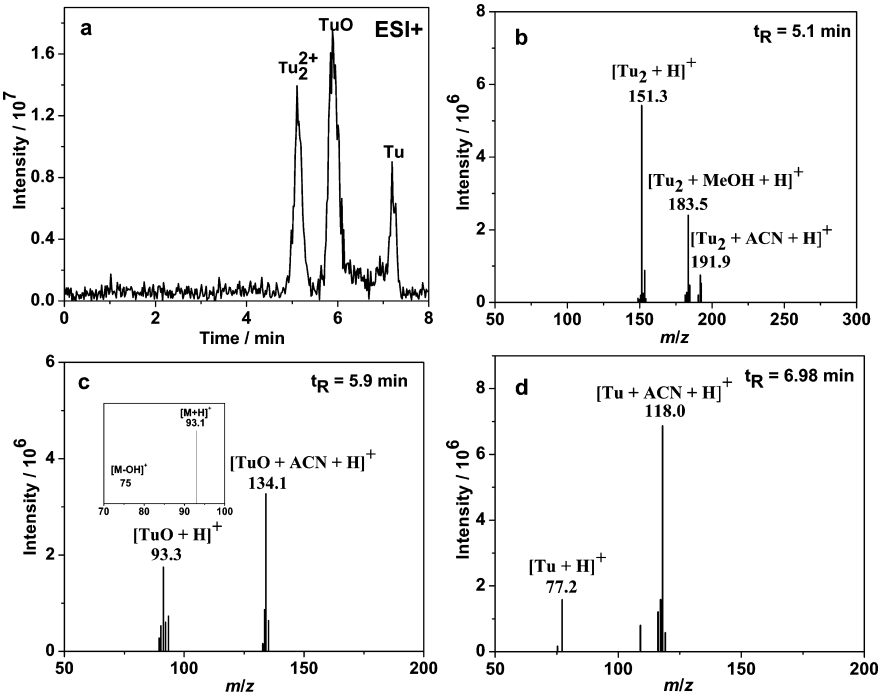


**Figure 6.** Total ions chromatogram and mass spectra of $H_2O_2$−Tu reaction system. (a) total ions chromatogram; (b−d) mass spectrum. Inset: MS/MS spectrum of $m/z$ 93.1. pH = 2.0, $[Tu]_0$ = 0.5 mM, $[H_2O_2]_0/[Tu]_0$ = 40:1, sampling at $t$ = 2 min, and $T$ = 25 °C.

**Table 2. Composite Reactions, Rate Laws, and Rate Constants of HPSTu**

| reactions | | |
|---|---|---|
| (M1) $H_2O \leftrightarrow H^+ + OH^-$ | | |
| (M2) $HSO_3^- \leftrightarrow H^+ + SO_3^{2-}$ | | |
| (M3) $H_2O_2 + HSO_3^- \rightarrow SO_4^{2-} + H^+ + H_2O$ | | |
| (M4) $H_2O_2 + SO_3^{2-} \rightarrow SO_4^{2-} + H_2O$ | | |
| (M5) $H_2O_2 + Tu \rightarrow TuO + H_2O$ | | |
| (M6) $Tu + TuO + 2H^+ \leftrightarrow Tu_2^{2+} + H_2O$ | | |
| (M7) $H_2O_2 + TuO \rightarrow TuO_2 + H_2O$ | | |
| (M8) $H_2O_2 + TuO_2 \rightarrow TuO_3 + H_2O$ | | |
| (M9) $H_2O_2 + TuO_3 \rightarrow SO_4^{2-} + OC(NH_2)_2 + H_2O + 2H^+$ | | |
| (M10) $TuO_3 + H_2O \rightarrow HSO_3^- + OC(NH_2)_2 + H^+$ | | |
| rate law | rate constants | ref |
| $v_1 = k_1[H_2O]$ | $k_1[H_2O]$ = 0.001 M $s^{-1}$ | 3 |
| $v_{-1} = k_{-1}[H^+][OH^-]$ | $k_{-1} = 1.0 \times 10^{11}$ $M^{-1}$ $s^{-1}$ | 3 |
| $v_2 = k_2\ [HSO_3^-]$ | $k_2$ = 3000 $s^{-1}$ | 3 |
| $v_{-2} = k_{-2}\ [H^+][SO_3^{2-}]$ | $k_{-2} = 5.0 \times 10^{10}$ $M^{-1}$ $s^{-1}$ | 3 |
| $v_3 = k_3[H_2O_2][HSO_3^-] + k_3'[H^+][H_2O_2][HSO_3^-]$ | $k_3$ = 4 $M^{-1}$ $s^{-1}$ | 4 |
| | $k_3'$ = 1.0 × 107 $M^{-2}$ $s^{-1}$ | 4 |
| $v_4 = k_4\ [H_2O_2][SO_3^{2-}]$ | $k_4$ = 0.2 $M^{-1}$ $s^{-1}$ | 9 |
| $v_5 = k_5[H_2O_2][Tu]$ | $k_5$ = 0.115 $M^{-1}$ $s^{-1}$ | 28 |
| $v_6 = k_6[TuO][Tu] + k_6'[Tu][TuO]\ [H^+]$ | $k_6$ = 0.5 $M^{-1}$ $s^{-1}$ | this work |
| $v_{-6} = k_{-6}[Tu_2^{2+}]$ | $k_6'$ = 1.3 × $10^6$ $M^{-2}$ $s^{-1}$ | this work |
| | $k_{-6}$ = 0.0011 $s^{-1}$ | this work |
| $v_7 = k_7[H_2O_2][TuO] + k_7'[H_2O_2][TuO][OH^-]$ | $k_7 = 1.28 \times 10^{-4}$ $M^{-1}s^{-1}$ | this work |
| | $k_7' = 1.092 \times 10^6$ $M^{-2}$ $s^{-1}$ | this work |
| $v_8 = k_8[H_2O_2][TuO_2]$ | $k_8$ = 0.0117 $M^{-1}$ $s^{-1}$ | 30 |
| $v_9 = k_9[H_2O_2][TuO_3]$ | $k_9$ = 0.0227 $s^{-1}$ | 30 |
| $v_{10} = k_{10}[TuO_3]$ | $k_{10} = 9.1 \times 10^{-6}$ $M^{-1}$ $s^{-1}$ | 30 |

oscillations. Moreover, bisulfite can also be produced by $TuO_3$ hydrolysis (M10). Since the rate constants of M8−M10 have no obvious influence on batch and CSTR simulations, here we adopted the rate constants by Gao et al.[30] at pH = 6.2, i.e., almost the average pH during oscillations. Figure 8a shows a calculated pH−time curve in batch. Comparison of the calculated curve with the measured one (Figure 1) demonstrates that our simulation is able to qualitatively reproduce the kinetic runs in batch. To simulate the kinetic behavior in the CSTR, we added appropriate flow terms to the model,


dx.doi.org/10.1021/jp500627z | J. Phys. Chem. A 2014, 118, 2702−2708

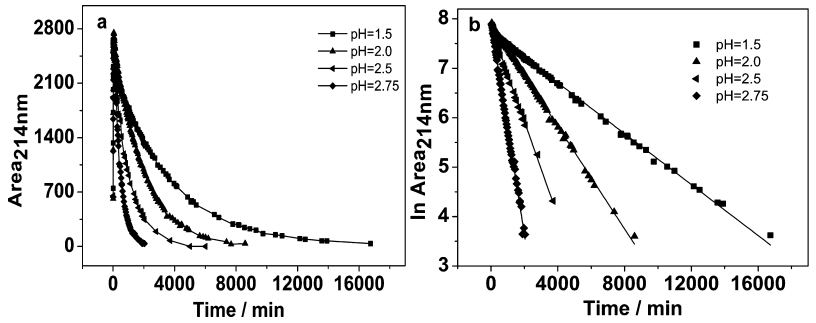


**Figure 7.** Kinetic curves and ln(area)−$t$ curves in the $H_2O_2$−Tu reaction. a, Kinetic curves of TuO; b, ln(area)−$t$ curves of TuO. $[Tu]_0$ = 0.5 mM, $[H_2O_2]_0$ = 20 mM, and $T$ = 25 °C.

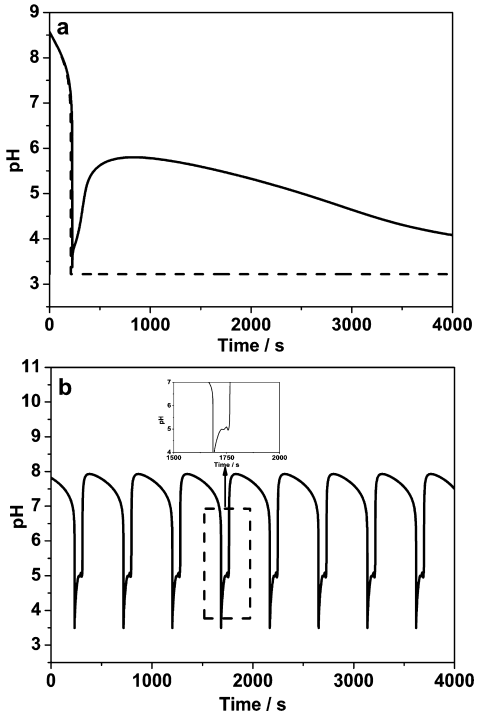


**Figure 8.** Calculated pH−time series under closed (a) and flow (b) conditions. Initial conditions are the same as Figures 1 and 2

including input and output flows for all the species. The calculated results are shown in Figure 8b. The model simulation obtained nearly quantitative agreement with the experimental pH oscillations in the flow system, including the irregular small-amplitude oscillations along the pH rising regime.

From the above discussion, in addition to bisulfite as a key species for proton positive feedback, another key species, TuO, is involved in reactions that consume proton at low pH and produce proton at high pH, giving two other feedback loops, resulting in complex pH oscillations in the HPSTu reaction system.

## 4. CONCLUSIONS

To summarize, in this work we observed oligo-oscillatory behavior in batch and large-amplitude regular pH oscillations in the HPSTu system under flow conditions. The mechanistic model including ten reactions can simulate the oscillatory behavior under flow conditions. With HPLC−MS, TuO was tracked as a long-lived species during the $H_2O_2$−Tu reaction in a broad pH range from acidic to neutral medium. Lower pH favors the reaction between Tu and TuO to get $Tu_2^{2+}$, resulting in a rise of pH, which is the proton negative feedback. On the contrary, higher pH quickens oxidation of TuO and hydrolysis of $Tu_2^{2+}$, inducing a decrease of pH, which is another proton negative feedback. Both regular pH oscillations and complex oscillations could be observed through coupling of proton positive feedback, i.e, bisulfite oxidation, and the two different negative feedbacks. Significantly, reactions involving TuO can consume or produce protons depending on pH, so TuO, in addition to bisulfite, is a key species for pH oscillations and complex oscillations. Our future studies will focus on detailed reactivity and kinetic parameters of TuO and spatiotemporal patterns of the system in reaction-diffusion media.

## AUTHOR INFORMATION

### Corresponding Author

*(Q.G.) E-mail: gaoqy@cumt.edu.cn.

### Notes

The authors declare no competing financial interest.

## ACKNOWLEDGMENTS

This work was supported by Grant 51221462 from the National Natural Science Foundation of China, the Fundamental Research Funds for the Central Universities (No. 2013XK05 and 2012LWB21), and PAPD. We acknowledge the friendly discussion of Prof. Attila Horváth and Prof. Sergei V. Makarov.

## REFERENCES

(1) Orbán, M.; Epstein, I. R. Systematic Design of Chemical Oscillators. 26. A New Halogen-free Chemical Oscillator: the Reaction between Sulfide Ion and Hydrogen Peroxide in a CSTR. *J. Am. Chem. Soc.* **1985**, *107*, 2302−2305.

(2) Rábai, G. Modeling and Designing of pH-controlled Bistability, Oscillations, and Chaos in a Continuous-flow Stirred Tank Reactor. *ACH—Models Chem.* **1998**, *135*, 381−392.

(3) Rábai, G.; Beck, M. T. High-Amplitude Hydrogen Ion Concentration Oscillation in the Iodate-Thiosulfate-Sulfite System under Closed Conditions. *J. Phys. Chem.* **1988**, *92*, 4831−4835.

(4) Rábai, G.; Szántó, T. G.; Kovács, K. Temperature-Induced Route to Chaos in the $H_2O_2$−$HSO_3^-$−$S_2O_3^{2-}$ Flow Reaction System. *J. Phys. Chem. A* **2008**, *112*, 12007−12010.

(5) Rabai, G. Period-Doubling Route to Chaos in the Hydrogen Peroxide−Sulfur(IV)−Hydrogen Carbonate Flow System. *J. Phys. Chem. A* **1997**, *101*, 7085−7089.

(6) Chie, K.; Okazaki, N.; Tanimoto, Y.; Hanazaki, I. Tristability in the Bromate−Sulfite−Hydrogencarbonate pH Oscillator. *Chem. Phys. Lett.* **2001**, *334*, 55−60.

(7) Edblom, E. C.; Orban, M.; Epstein, I. R. A New Iodate Oscillator: the Landolt Reaction with Ferrocyanide in a CSTR. *J. Am. Chem. Soc.* **1986**, *108*, 2826−2830.
(8) Edblom, E. C.; Luo, Y.; Orbán, M.; Kustin, K.; Epstein, I. R. Systematic Design of Chemical Oscillators. 45. Kinetics and Mechanism of the Oscillatory Bromate-Sulfite-Ferrocyanide Reaction. *J. Phys. Chem.* **1989**, *93*, 2722−2727.
(9) Rábai, G.; Kustin, K.; Epstein, I. R. A Systematically Designed pH Oscillator: the Hydrogen Peroxide−Sulfite−Ferrocyanide Reaction in a Continuous-Flow Stirred Tank Reactor. *J. Am. Chem. Soc.* **1989**, *111*, 3870−3874.
(10) Rábai, G.; Nagy, Z. V.; Beck, M. T. Quantitative Description of the Oscillatory Behavior of the Iodate−Sulfite−Thiourea System in CSTR. *React. Kinet. Catal.* **1987**, *33*, 23−29.
(11) Okazaki, N.; Rábai, G.; Hanazaki, I. Discovery of Novel Bromate−Sulfite pH Oscillators with $Mn^{2+}$or $MnO_4^-$ as a Negative-Feedback Species. *J. Phys. Chem. A* **1999**, *103*, 10915−10920.
(12) Rábai, G.; Beck, M. T. Oxidation of Thiourea by Iodate: a New Type of Oligo-oscillatory Reaction. *J. Chem. Soc., Dalton. Trans.* **1985**, 1669−1672.
(13) Simoyi, R. H. New Bromate Oscillator: the Bromate−Thiourea Reaction in a CSTR. *J. Phys. Chem.* **1986**, *90*, 2802−2804.
(14) Alamgir, M.; Epstein, I. R. Systematic Design of Chemical Oscillators. Part 25. Complex Dynamical Behavior in a New Chemical Oscillator: The Chlorite−Thiourea Reaction in a CSTR. *Int. J. Chem. Kinet.* **1985**, *17*, 429−439.
(15) Liu, H.; Horváth, A. K.; Zhao, Y.; Lv, X.; Yang, L.; Gao, Q. A Rate Law Model for the Explanation of Complex pH Oscillations in the Thiourea−Iodate−Sulfite Flow System. *Phys. Chem. Chem. Phys.* **2012**, *14*, 1502−1506.
(16) Lee, K. J.; McCormick, W. D.; Ouyang, Q.; Swinney, H. L. Pattern Formation by Interacting Chemical Fronts. *Science* **1993**, *261*, 192−194.
(17) Horváth, J.; Szalai, I.; De Kepper, P. An Experimental Design Method Leading to Chemical Turing Patterns. *Science* **2009**, *324*, 772−775.
(18) Horváth, J.; Szalai, I.; De Kepper, P. Pattern Formation in the Thiourea−Iodate−Sulfite System: Spatial Bistability, Waves, and Stationary Patterns. *Phys. D* **2010**, *239*, 776−784.
(19) Rábai, G. pH-Oscillations in a Closed Chemical System of $CaSO_3$−$H_2O_2$−$HCO_3^-$. *Phys. Chem. Chem. Phys.* **2011**, *13*, 13604−13606.
(20) Poros, E.; Horváth, V.; Kurin-Csoergei, K.; Epstein, I. R.; Orbán, M. Generation of pH-Oscillations in Closed Chemical Systems: Method and Applications. *J. Am. Chem. Soc.* **2011**, *133*, 7174−7179.
(21) Pikovsky, A.; Rosenblum, M. Partially Integrable Dynamics of Hierarchical Populations of Coupled Oscillators. *Phys. Rev. Lett.* **2008**, *101*, 264103.
(22) Abrams, D.; Mirollo, R.; Strogatz, S.; Wiley, D. Solvable Model for Chimera States of Coupled Oscillators. *Phys. Rev. Lett.* **2008**, *101*, 084103.
(23) Omelchenko, I.; Omel'chenko, O. E.; Hövel, P.; Schöll, E. When Nonlocal Coupling between Oscillators Becomes Stronger: Patched Synchrony or Multichimera States. *Phys. Rev. Lett.* **2013**, *110*, 224101.
(24) Kuksenok, O.; Dayal, P.; Bhattacharya, A.; Yashin, V. V.; Deb, D.; Chen, I. C.; Van Vliet, K. J.; Balazs, A. C. Chemo-Responsive, Self-Oscillating Gels that Undergo Biomimetic Communication. *Chem. Soc. Rev.* **2013**, *17*, 7257−7277.
(25) Frerichs, G. A.; Thompson, R. C. A pH-Regulated Chemical Oscillator: The Homogeneous System of Hydrogen Peroxide−Sulfite−Carbonate−Sulfuric Acid in a CSTR. *J. Phys. Chem. A* **1998**, *102*, 8142−8149.
(26) Szalai, I.; Horvath, J.; Takacs, N.; De Kepper, P. Sustained Self-organizing pH Patterns in Hydrogen Peroxide Driven Aqueous Redox Systems. *Phys. Chem. Chem. Phys.* **2011**, *13*, 20228−20234.
(27) Szalai, I.; Cuinas, D.; Takacs, N.; Horváth, J.; De Kepper, P. Chemical Morphogenesis: Recent Experimental Advances in Reaction−Diffusion System Design and Control. *Interface Focus* **2012**, *2*, 417−432.
(28) Hoffmann, M.; Edwards, J. O. Kinetics and Mechanism of the Oxidation of Thiourea and *N,N′*-Dialkylthioureas by Hydrogen Peroxide. *Inorg. Chem.* **1977**, *16*, 3333−3338.
(29) Gao, Q.; Wang, G.; Sun, Y.; Epstein, I. R. Simultaneous Tracking of Sulfur Species in the Oxidation of Thiourea by Hydrogen Peroxide. *J. Phys. Chem. A* **2008**, *112*, 5771−5773.
(30) Gao, Q.; Liu, B.; Li, L.; Wang, J. Oxidation and Decomposition Kinetics of Thiourea Oxides. *J. Phys. Chem. A* **2007**, *111*, 872−877.
(31) Arifoglu, M.; Marmer, W. N.; Dudley, R. L. Reaction of Thiourea with Hydrogen Peroxide: $^{13}C$ NMR Studies of an Oxidative/Reductive Bleaching Process. *Textile Res. J.* **1992**, *62*, 94−100.
(32) Giannos, S. A.; Dinh, S. M.; Berner, B. Polymeric Substitution in a pH Oscillator. *Macromol. Rapid Commun.* **1995**, *16*, 527−531.
(33) Giannos, S. A.; Dinh, S. M.; Berner, B. Temporally Controlled Drug Delivery Systems: Coupling of pH Oscillators with Membrane Diffusion. *J. Pharm. Sci.* **1995**, *84*, 539−543.
(34) Liedl, T.; Simmel, F. C. Switching the Conformation of a DNA Molecule with a Chemical Oscillator. *Nano Lett.* **2005**, *5*, 1894−1898.
(35) Liedl, T.; Sobey, T. L.; Simmel, F. C. DNA-Based Nanodevices. *Nano Today* **2007**, *2*, 36−41.
(36) Rio, L. G.; Munkley, C. G.; Stedman, G. Kinetic Study of the Stability of $(NH_2)_2CSSC(NH_2)^{2+}$. *J. Chem. Soc., Perkin Trans.* **1996**, *5*, 159−162.